

Optimization of biomass composition explains microbial growth-stoichiometry relationships

Oskar Franklin¹, Edward K. Hall², Christina Kaiser³, Tom J. Battin², Andreas Richter³

¹ IIASA International Institute for Applied Systems Analysis, A-2361 Laxenburg, Austria. franklin@iiasa.ac.at (corresponding author), ² University of Vienna, Department of Limnology, Althanstrasse 14, A-1090, Vienna, Austria, ³ University of Vienna, Department of Chemical Ecology, Althanstrasse 14, A-1090, Vienna, Austria

ABSTRACT: Integrating microbial physiology and biomass stoichiometry opens far reaching possibilities for linking microbial dynamics to ecosystem processes. For example, the growth rate hypothesis (GRH) predicts positive correlations among growth rate, RNA content and biomass phosphorus (P) content. Such relationships have been used to infer patterns of microbial activity, resource availability and nutrient recycling in ecosystems. However, for microorganisms it is unclear under which resource conditions the GRH applies. We developed a model to test if the response of microbial biomass stoichiometry to variable resource stoichiometry can be explained by a trade-off among cellular components that maximizes growth. The results show mechanistically why the GRH is valid under P-limitation but not under N-limitation. We also show why variability of growth rate – biomass stoichiometry relationships is lower under P- than under N- or C limitation. These theoretical results are supported by experimental data on macromolecular composition (RNA, DNA and protein) and biomass stoichiometry from two different bacteria. In addition, compared to a model with strictly homeostatic biomass, the optimization mechanism we suggest results in increased microbial N and P mineralization during organic matter decomposition. Therefore this mechanism may also have important implications for our understanding of nutrient cycling in ecosystems.

Keywords: optimization model, mineralization, growth rate hypothesis, RNA, biomass stoichiometry, microbial physiology

Introduction

Ecological stoichiometry provides a powerful tool for integrating microbial physiology and stoichiometry with ecosystem processes. For example, the growth rate hypothesis (GRH) predicts that growth rate increases with phosphorous concentration through changes in RNA content (Sterner 1995), which has been observed in organisms from microbes (Makino et al. 2003) to humans (Elser et al. 2007). Recent theoretical advances show that the GRH coupled with the metabolic theory

of ecology can explain stoichiometric patterns across organism types (Allen and Gillooly 2009). The GRH also underlies the basis for experimental methods to estimate microbial activity based on rRNA content (Leser et al. 1995). However, these methods and theories should be interpreted with care as observations (Binder and Liu 1998; Elser et al. 2003; Flårdh et al. 1992) show that the GRH is not universally valid, especially in microorganisms. Relationship between bacterial biomass stoichiometry and growth rate can vary within the same species (Chrzanowski and Grover 2008; Chrzanowski and Kyle 1996; Makino et al. 2003) and depend on which nutrient is limiting growth (Sepers 1986). The mechanisms behind this variability are not yet well understood. Moreover, it has been proposed that a general lack of theory limits the progress in the field of microbial ecology (Prosser et al. 2007). Thus, developing theory and models is an important step in elucidating the mechanisms behind the variable stoichiometry of microorganisms and its implications for nutrient cycling in ecosystems.

The response of microbial growth to variation in resource stoichiometry has commonly been modeled using cellular quotas, i.e. the Droop model (Droop 1968; Thingstad 1987). A phytoplankton model by Klausmeier et al. (2004) also based on quotas took this approach one step further by adding mechanistic detail linking the minimum quotas to structural composition in terms of resource acquisition and growth machinery. More importantly, this model employed optimization strategy of trade-offs between resource acquisition machinery and growth machinery to control biomass composition. Optimality assumptions are attractive because they provide an ecological (and/or evolutionary) rationale for model behavior. Whereas optimal biomass allocation principles have been widely used to explain the response of plants and animals to resource availability (e.g. Franklin et al. 2009; Kozłowski et al. 2004), the few such studies that have been conducted for microorganisms are (to our knowledge) restricted to phytoplankton (e.g. Klausmeier et al. 2004; Wirtz 2002). For bacteria, proteome studies suggest trade-offs among growth and nutrient

acquisition (e.g. Raman et al. 2005). However, the hypothesis that optimal allocation of cellular machinery explains the response of growth rate and biomass stoichiometry to resource stoichiometry in heterotrophic microorganisms has yet to be tested.

Here we take the optimization approach (Klausmeier et al. 2004) one step further in terms of mechanistic detail by explicitly modeling the growth process as a function of internal resource pools and cellular growth and uptake machinery, each with a fixed elemental composition. We hypothesize an optimal partitioning of biomass among growth machinery, uptake machinery and other structural biomass. We then evaluate how optimization among these components affects biomass composition and stoichiometry under variable resource stoichiometry. Specifically we show that (1) optimization of biomass composition that maximizes specific growth rate explains variability in bacterial biomass stoichiometry, (2) resource stoichiometry strongly influences macromolecular composition (e.g. RNA content) so that the GRH is valid under P- but not N limitation, and (3) the presence of an optimization

mechanism increases P and N recycling under C limited bacterial growth compared to if biomass was strictly homeostatic.

Theory and model

Model structure and the optimal biomass composition hypotheses

In our model, structural biomass (fig. 1, Table 1) is divided into different cellular compartments with specific functions: 1) baseline biomass, denoted as z (DNA, cellular membrane, cell wall, essential proteins), 2) growth machinery g (ribosomes, RNA), and 3) uptake machinery u (transmembrane proteins). In addition to structural biomass, we consider internal C, N and P metabolite pools that are used for growth and respiration. All processes and variables (described below; Table 2) are defined on a per biomass basis, which allows us to not explicitly consider effects of cell volume or density changes. Unless indicated, biomass refers to the structural biomass only (excluding the internal metabolite pools).

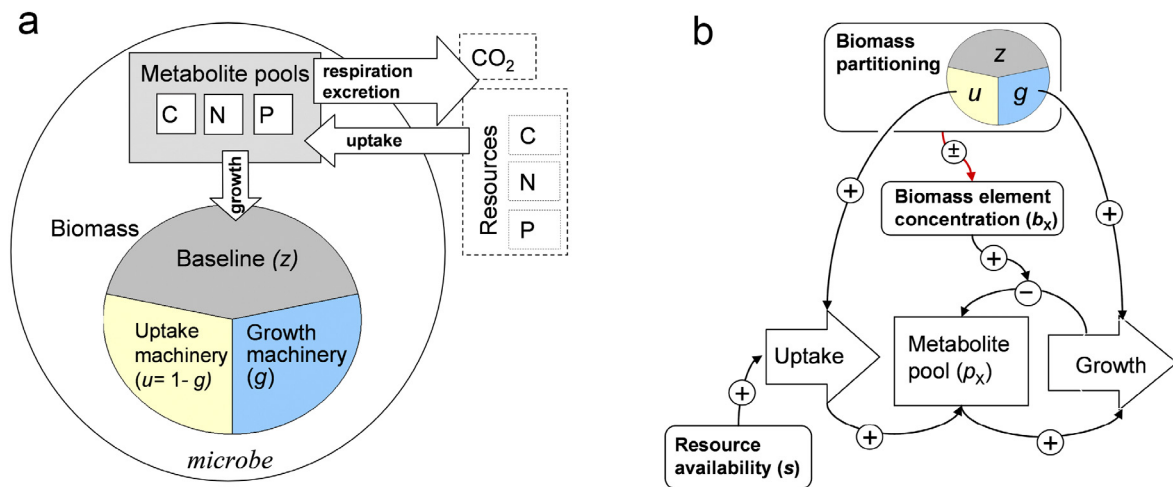


Fig. 1. Model structure. (a) Model components and fluxes (processes) (b) The effect of biomass partitioning on cell processes for a growth limiting element. Arrows indicate positive (+), negative (-) and a variable (\pm) effect. Biomass composition (u , g , and z) has direct functional effects on growth and uptake and an indirect effect through biomass element concentration that affects nutrient metabolite consumption per unit of biomass growth (nutrient use efficiency). For clarity, excretion (which is negligible for a limiting element) and respiration (which is constant) are not shown.

For a given resource level (s) the relative partitioning of biomass among the three cell compartments (uptake machinery u , growth machinery g , and baseline biomass z) is adjusted to maximize the specific growth rate (G). Specifically, the optimal cell composition depends on

the balance between growth and uptake capacity and is further influenced by the elemental (C, N, P) demand for the construction of the selected biomass composition (fig. 1b). The fraction of baseline biomass z is however assumed to always be greater than a minimum value z_{\min}

to maintain essential functions other than growth and uptake. Adjustments of biomass composition, e.g. amount of RNA, have been shown to occur rapidly in response to environmental changes and in experiments (Ferenci 2007; Kerkhof and Kemp 1999). Thus, we

assume that biomass composition is in dynamic equilibrium with the environmental conditions, although we also evaluate under which resource conditions the biomass composition may deviate from the optimal equilibrium based predictions.

Table 1. Composition of cell compartments

Cell compartment	Symbol	Composition	Protein	C	N	P
Baseline biomass	z	cell wall, membranes, DNA (15, 17) ⁴	62, n.d. ⁴	43	14.9, 13.7 ⁴	1.0, 1.0 ⁴
Uptake machinery	u ³	protein	100	46	17	0
Growth machinery	g ³	Ribosomal protein (33), RNA (67) ¹	33	37	15.3	5.87
C in metabolites	p_C	carbohydrates (50), lipids (50)	0	54.2 ²	0	0
N in metabolites	p_N	NH ₄ (50), amino acids (50)	0	23	47.4	0
P in metabolites	p_P	NaPO ₄ (50), NaPO ₃ (50)	0	0	0	28

All values in percent mass. Unless indicated, C N P % in macro molecules and cell compartments are taken from Sterner and Elser (2002).

¹assuming 85% of RNA is in ribosomes and ribosome RNA/ protein = 1.8 for prokaryotes (Sterner and Elser 2002).

²(Vrede et al. 2004).

³Mathematically, u and g are the uptake and growth fractions, respectively, of the non-baseline biomass (1- z).

⁴Estimated from data for *P. carotovorum* and *E. coli*, respectively. n.d. = not determined.

Table 2. Variables and parameters

Symbol	Unit	Values ¹	Description
<i>variables</i>			
b_X	$gX gB^{-1}$	-	fraction of element X in biomass
E_X	$gX gB^{-1}h^{-1}$	-	specific rate of excretion of element X
g	-	-	fraction non baseline biomass in growth machinery
G	h^{-1}	-	specific growth rate
p_X	$gX gB^{-1}$	-	metabolite pool of element X
U_X	$gX gB^{-1} h^{-1}$	-	resource uptake U of element X
u	-	-	fraction non baseline biomass in uptake machinery
s_X	$gX gB^{-1} h^{-1}$	-	external resource level of element X.
z	-	-	fraction baseline biomass of total structural biomass
<i>parameters</i>			
e_g	-	<i>P.c.</i> : 0.38, <i>E.c.</i> : 56	maximum efficiency of the growth machinery
f_E	-	0.01	excretion rate factor
f_G	h^{-1}	<i>P.c.</i> : 0.93, <i>E.c.</i> : 4.2	maximal synthetic capacity of the growth machinery
p_{limX}	$gX gB^{-1}$	<i>P.c.</i> : 0.43, 0.10, 0.021 <i>E.c.</i> : 0.42, 0.029, 0.0085	Theoretical maximum metabolite pools of C, N, and P, respectively
r	$gC gB^{-1} h^{-1}$	0.2 ²	specific maintenance respiration
y	-	0.5 ³	growth efficiency, C growth per C used in the growth process
z_{min}	-	<i>P.c.</i> : 0.56, <i>E.c.</i> : 0.19	minimum fraction baseline biomass of total structural biomass

B = structural biomass (biomass excluding the nutrient metabolite pools).

X denotes any of the elements C, N or P.

¹*P.c.*, *E.c.* = *P. carotovorum* and *E. coli*, respectively

All parameter values estimated from our data except ²(Tännler et al. 2008) and ³(Cajal-Medrano and Maske 1999).

Cellular compartments and stoichiometry

The elemental composition of each cellular compartment (Table 1) is based on values derived from the literature and original research presented in this study (see below). Only the elements C, N and P are

explicitly modeled whereas all other atoms in biomass and metabolites are implicit. Specifically, the proportion of element X in biomass (b_X ; where X denotes C, N or P), is the product of relative amount of

each cellular compartment and its elemental content (X_g, X_u, X_z , eq. 1).

$$\begin{aligned} b_X &= z(X_z) + (1-z)(gX_g + uX_u) = \\ z(X_z) + (1-z)(gX_g + (1-g)X_u) \end{aligned} \quad (\text{eq. 1})$$

In eq. 1, g and u are defined as fractions of the non-baseline biomass so that $u = 1-g$. Resources are taken up from the environment and stored in metabolite pools that are represented by their C, N and P content although the actual chemical forms of the resource pools (metabolites) are variable, e.g. carbohydrates (C), amino acids (N,C), and phosphates (P). Nutrients are tapped from the metabolite pools (p) for growth of new biomass (G) and respiration (R), or excreted (e.g. overflow metabolism; E). Metabolite pools are assumed to be in dynamic equilibrium, so that their size

depends on the balance between nutrient uptake (U) and use (eq 2).

$$\begin{aligned} dp_X/dt &= U_X - G b_X - E_X = 0, \quad \text{where } X = \text{N or P (eq. 2)} \\ dp_C/dt &= U_C - G b_C - E_C - R = 0 \end{aligned}$$

Cell processes –growth, uptake, respiration and excretion

Growth

The growth model is based on the synthesizing unit (SU) concept, which is based on the microscopic interactions of growth machinery and different nutrients (Appendix A, Kooijman 1998, Kooijman 2001). In our framework the SU concept leads to a growth equation (eq. 3) where G increases with the ratio of metabolite concentration (p_X) to the demand of the same nutrient for biomass growth (controlled by b_X) until G approaches its maximum G_{max}

$$\frac{db}{dt} \frac{1}{b} = G = \frac{G_{max}}{1 + \frac{G_{max}}{e_g} \left[\frac{b_C}{p_C} + \frac{b_N}{p_N} + \frac{b_P}{p_P} - \left(\frac{p_C}{b_C} + \frac{p_N}{b_N} \right)^{-1} - \left(\frac{p_C}{b_C} + \frac{p_P}{b_P} \right)^{-1} - \left(\frac{p_P}{b_P} + \frac{p_N}{b_N} \right)^{-1} + \left(\frac{p_C}{b_C} + \frac{p_N}{b_N} + \frac{p_P}{b_P} \right)^{-1} \right]} \quad (\text{eq. 3})$$

In eq. 3, e_g is the initial efficiency of the SU, i.e. the growth per metabolite availability at low metabolite concentration (p_X). G_{max} (maximum G , eq. 4) is proportional to the amount of growth machinery g ($1-z$) and its maximum capacity of biomass synthesis (f_G), which is a function of the maximal translational activity of the ribosomes (cf. Jackson et al. 2008).

$$G_{max} = f_G(1-z)g \quad (\text{eq. 4})$$

It is commonly assumed that a single nutrient limits growth (cf. Liebig's law). In our model this means that for the limiting nutrient, the ratio of the metabolite pool (p_X) to biomass concentration (b_X) is much smaller than for the non-limiting nutrients. Under these circumstances eq. 3 can be approximated by eq. 5 which more clearly illustrates the interaction of G_{max} and each metabolite pool, i.e. why small metabolite pools limit growth whereas G_{max} limits growth when metabolite pools are large.

$$G = \frac{G_{max}}{1 + \frac{G_{max}}{e_g} \frac{b_X}{p_X}} \quad (\text{eq. 5})$$

In eq. 5, X refers to the most limiting nutrient.

Uptake

Similar to the growth dynamics limited by G_{max} , resource uptake (U , eq. 6) is limited by uptake capacity (U_{max}) at high external resource level (s), whereas it is limited by s at low s (cf. Brandt et al. 2004; i.e. a Jacob Monod or Michaelis-Menten type functional form).

$$U_X = \frac{U_{max X} s_X}{U_{max X} + s_X} \quad (\text{eq. 6})$$

U_{max} is a function of uptake machinery (u) as defined below. As we consider external resources solely regarding their total effects on potential rate of element uptake we can neglect underlying details of the uptake response to s , such as effects of different resource types. Instead s represents the total effect of resource level on uptake, i.e. s_X is the uptake of element X when the limitation by U_{max} is removed and U is completely resource limited. Uptake of a non-limiting element is approximated by $U = U_{max}$ in our simulations.

Excretion and respiration

To avoid that any element reach an unrealistic or deleterious concentration there is an upper limit to the size of each internal nutrient pool (p) (Russell and Cook 1995). If p approaches its upper limit (p_{lim}) nutrients are

excreted, rejected (for P and N) or respired (for C, overflow respiration) according to eq. 7 (fig. B1, Online Appendix B).

$$E_X = \frac{f_E P_X}{P_{\text{lim}X} - P_X} \quad (\text{eq. 7})$$

In eq. 7, f_E controls how quickly E increases with p and is assumed to be low ($f_E = 0.01$) so that E is minimal below $p \rightarrow p_{\text{lim}}$.

Anabolic respiration associated with the construction of biomass (R_G) is proportional to growth (G), i.e. $R_G = y G$ where y is the growth efficiency ($y = \text{biomass C growth} / \text{total C used in the growth process}$). Although y may be variable among species and for different environmental conditions, differences in y have only quantitative effects under C limitation but no qualitative effects on our results. Thus for simplicity we assume a growth efficiency of $y=0.5$ (Cajal-Medrano and Maske 1999). Specific maintenance respiration (R_m) is assumed to be constant for each species (Pirt 1982), but varies among species. A linear relationship between maximum G and specific maintenance rate (R_m) has been observed across species (Van Bodegom 2007), which can be explained by the energetic costs of protein synthesis machinery (here g) increasing with its translation speed (here f_G) (Dethlefsen and Schmidt 2007). In our model this relationship corresponds to R_m proportional to f_G (eq. 8), where $r = 0.02$ (Tännler *et al.* 2008) is the baseline respiration.

$$R_m = r f_G \quad (\text{eq. 8})$$

Balancing capacities for nutrient uptake and use

Uptake capacity and growth capacity are linked to their respective proportions (g and u) of the non-base line biomass ($1-z$) through a trade-off ($u = 1-g$) so that both capacities cannot be maximized simultaneously. Furthermore, based on the benefits of the ability to utilize and buffer variations in resource supply (e.g. Thomas and O'Shea 2005) maximum uptake capacity should be higher than maximum growth capacity. Specifically, we assume that a reference uptake capacity, given by $u=u_0=0.5$, suffices to match maximum growth capacity (U_{max} at $g = u = 0.5$ equals $G_{\text{max}} b_X$ at $g = 1$) for each nutrient, which leads to eq. 9. However, as long as the maximum uptake capacity is not smaller than maximum growth capacity, our results are not sensitive to this assumption.

$$U_{\text{max}X} = \frac{f_G b_X}{u_0} u (1-z) \quad \text{for } X = \text{N or P}$$

$$U_{\text{max}C} = \left(\frac{f_G b_C (1-z_{\text{min}})}{y} + r f_G \right) \frac{u(1-z)}{(1-z_{\text{min}})u_0} \quad (\text{eq. 9})$$

In eq. 9, b_X (eq. 1) is evaluated at $g = u_0 = 0.5$ and $z = z_{\text{min}}$.

Model evaluation

Solving for optimal biomass composition

To evaluate the model, G (eq. 3) was maximized with respect to biomass composition (g and z) for each substrate level (s), under the constraint $z > z_{\text{min}}$. We numerically solved for s to obtain optimal g and z as a function of G . In each case single element limitation was modeled, i.e. only one resource element at a time affected G while the effects of the other resources were fixed by setting their uptake rate $U = U_{\text{max}}$ (see *Uptake*). In addition we evaluated the robustness of the optimal biomass composition in terms of the probability for sub-optimal values of g and z . For example, due to rapid fluctuations in resource level cells may not always be in dynamic equilibrium with the environment and may therefore deviate from the modeled optimal composition, which would lead to variation around the optimal $G - g - z$ relationships. The range of this variability should be larger the less sensitive G is to deviation of g and z from their respective optima. Thus, as a measure of potential variability in g and z we calculated how far each parameter can be from the optima without reducing G more than 5 percent.

Model testing and evaluation

To test the most central assumption in the model, optimal biomass partitioning, we compared model predictions and data for concentrations of macromolecules specific for two of the three biomass compartments. The data came from a chemostat experiment: *E. coli* (Makino *et al.* 2003), and a batch culture experiment using *Pectobacterium carotovorum* (Online Appendix C; Keiblinger *et al.* 2010). RNA was used as an index of growth machinery (as 85% amount of cellular RNA is ribosomal rRNA – Table 1) and DNA was used as an index of baseline biomass. To minimize the effect of changes in non-structural components, i.e. metabolite pools, we analyzed RNA and DNA relative to protein content (for *P. carotovorum*), which is not affected by metabolite pools. When protein data was not available (for *E. coli*) it was replaced by total N content. The model was fitted (see method below) to measured RNA:protein, DNA:protein, and P metabolite pool: protein for *P. carotovorum* and RNA:N and DNA:N for *E. Coli*. For the testing of metabolite pool dynamics we chose P because for P we can more easily separate metabolites and structural components, i.e. in RNA (fixed proportion of growth machinery) and in baseline

biomass (constant under P limitation; Table 1), than for C and N that occur in all cell compartments and in more than one metabolite pool each. For *P. carotovorum*, the limiting nutrient was identified for each treatment based on measured dynamics of metabolite pools and storage (polyphosphate and carbohydrates) in response to growth rate (Online Appendix C). For *E. coli* we relied

Parameterization

Although the elemental composition of macromolecules and the macromolecular composition of the cellular compartments are constrained (Sterner and Elser 2002), some components vary among species or are difficult to estimate accurately based on literature data. Thus we estimated species specific values for minimum baseline biomass (z_{\min}) and its N, protein and DNA content based on data for each species. For the process related parameters we estimated species-specific values for maximum capacity (f_G) and efficiency (e_g) of the growth machinery and maximum metabolite pool sizes ($p_{\text{lim}X}$). Best fit parameters (maximum likelihood of yielding the measured data) were estimated using Markov Chain Monte Carlo (MCMC; e.g. Gelman et al. 2004), which has the advantage, compared to standard optimum seeking methods, of minimizing the risk of selecting a local but not global optimum for the parameter values. For all calculations we used MathCad (version 13) software (files in Online Appendix D).

Results – model performance and behavior

Modelled and measured relationships between growth rate and macromolecular biomass composition

In order to evaluate the presence of the hypothesized optimization mechanism, we compared measurements with model predictions (optimal and potential sub-optimal ranges of variability) of co-variation of biomass composition and specific growth rate, induced by variation in resource level and resource C:N:P stoichiometry. Specifically, we tested for RNA: protein, DNA: protein, and P-metabolite pools: protein ratios under N and P limitation for *P. carotovorum*. For *E. coli* protein data were not available so we tested for RNA:N and DNA:N under C and P limitation.

For *P. carotovorum* the modeled biomass composition versus growth rate (G) differed significantly between N limited growth and P limited growth (fig. 2). Under P limitation modeled RNA: protein increased linearly with G in accordance the growth rate hypothesis (GRH). However, under N limitation the modeled RNA: protein relationship with G was non-linear and clearly defied the GRH. Also the modeled DNA: protein ratio differed between P and N limitation. Whereas this ratio did not

on limitations identified in the original study (Makino et al. 2003). Finally, we evaluated the consequences of our optimization hypothesis for nutrient recycling during decomposition by simulating the effect of declining resource C availability, which is ubiquitous during organic matter decomposition.

vary with G under P limitation it increased with declining G under N limitation, resulting from a relative increase in baseline biomass (z , which includes DNA) and a relative reduction of both growth and uptake machinery. These model predictions of optimal biomass composition were consistent with the observed trends in RNA: DNA: protein ratios versus G , capturing the differences in these relationships between P and N limitation (fig. 2). In addition, most of the observed variability of the response variables was within the modeled range of potential variability (thin lines in fig.2), although under P limitation some observed variability in DNA: protein could not be readily explained by the model. For *E. coli* the model predicted linearly increasing RNA:N versus G under P limitation and a similar relationship with smaller slope under C limitation over the range of observed G s. For optimal DNA:N no effect of G or difference between C and P limitation was predicted by the model. However, for both DNA:N and RNA:N the model suggests a higher potential variability under C than under P limitation. These modeled trends for optimal biomass composition were again consistent with the observations (fig. 2).

Modeled P metabolite pool in *P. carotovorum* differed significantly between P limited and non P limited conditions, resulting in a much lower pool under P- than under N limitation (fig. 3). In addition, under P limitation the P metabolite pool increased strongly with increasing G whereas such a monotonic relationship was not present under N limitation. The model implies that this difference reflects a general difference between the metabolite pool dynamics of limiting and non-limiting nutrients. For a limiting nutrient the metabolite pool (p) increases with G because p is a dominant control of G . (fig. 1b, eq. 5). In contrast, non-limiting nutrients can accumulate in metabolite pools without strong effects on G . Instead, non limiting metabolites are passively controlled by the flux balance of the cell, for example, they are reduced through increased use when G increases at constant uptake capacity. This difference between limiting and non-limiting conditions was confirmed by the measured trends in P metabolites in *P. carotovorum* (fig. 3).

The differences in estimated model parameters (the model interpretation of the empirical data) between the two bacterial species imply that *E. coli* reaches a higher G than *P. carotovorum* due to its higher capacity (f_G) and higher efficiency (e_g) of its growth machinery. The difference in G is further enhanced by *E. coli*'s lower

minimum requirement for baseline biomass (z_{min}). The model also suggested that the species differed in their maximum metabolite pools for P and N, although we were not able to evaluate this based on the available empirical data.

In summary, the model predicted the trends in the relationships among biomass G , RNA, DNA and protein

and how those relationships differed under C, N and P limitation in agreement with observations. This result is consistent with an optimization of biomass composition to maximize specific growth rate in response to resource levels. In addition, the agreement between modeled and measured dynamics of the metabolite pools was consistent with the growth and uptake mechanisms proposed in the model.

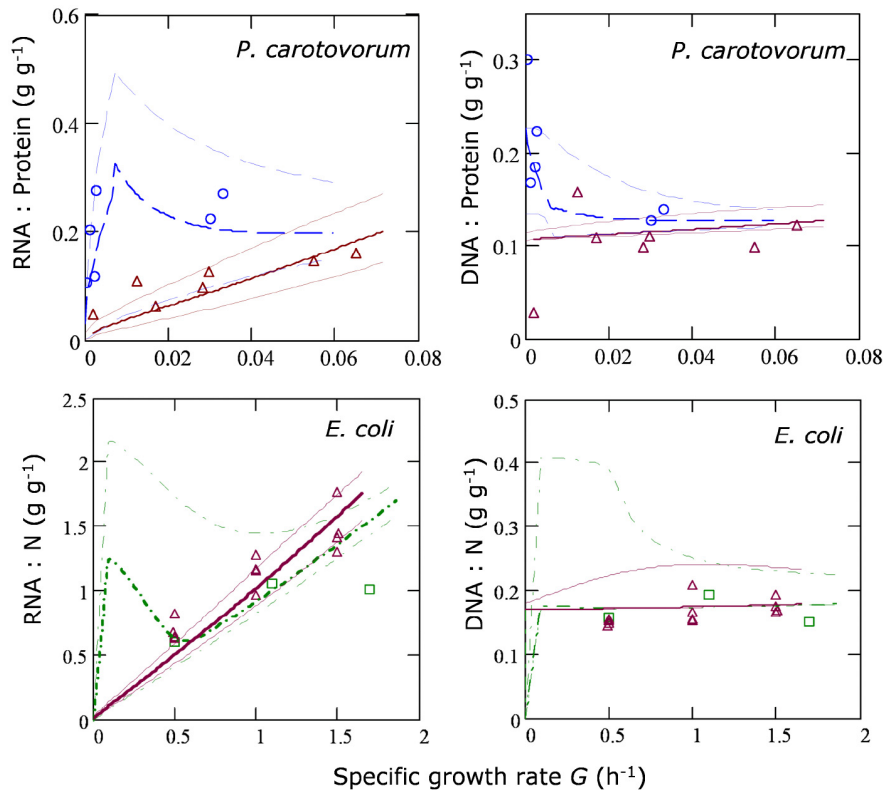


Fig. 2. Relationships between biomass composition ratios and specific growth rate (G) induced by variation in external resource levels for two species of bacteria. Modeled (lines) and measured (symbols) results for growth under different single element limitations: N limitation (dashed lines, circles), P limitation (solid lines, triangles), and C limitation (dash-dot lines, squares). The optimal state (middle thick line) and intervals of near-optimal states (95% optimal, upper and lower thin lines) were modeled. The distance between the thin lines represents the range of near optimal values. For *P. carotovorum* $r^2 = 0.79, 0.10$ for RNA:protein and DNA:protein, respectively under P limitation, and $0.43, 0.63$ under N limitation. For *E. coli* $r^2 = 0.86, 0.31$ for RNA:N and DNA:N, respectively under P limitation, and $0.57, 0.086$ under C limitation.

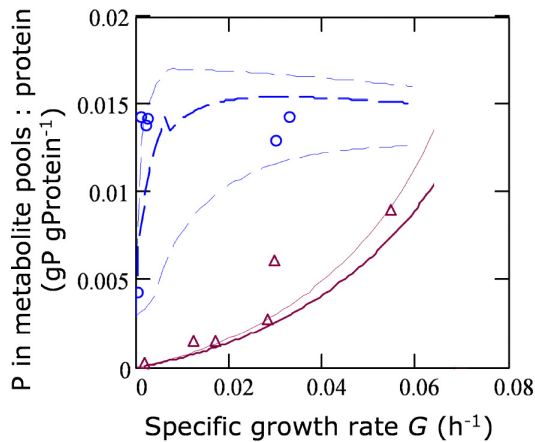


Fig. 3. Relationships between metabolite pool phosphorus: biomass protein ratio and specific growth rate (G) induced by variation in external resource levels. The growth limiting elements were nitrogen (N) or phosphorus (P) (Symbols and lines as in fig. 2). The lower thin solid line for P limitation (near-optimal values) coincides with the thick solid line (optimal values). Measured P metabolite pools were calculated from the P budget as $P_{\text{total}} - P_{\text{RNA}} - P_z$, where $P_z = P_{\text{DNA}} + P_{z \text{ non-DNA}}$. $P_{z \text{ non-DNA}}$ was the non-DNA P content in baseline biomass (z) was estimated to 0.28% by fitting the y-intercept of the metabolite pool versus G under P limitation to 0. For P limitation, one outlier at $G=0.065$ for which the estimated P metabolite pool was below 0 was removed from the analysis. $r^2=0.32$ and 0.87 under N and P limitation, respectively.

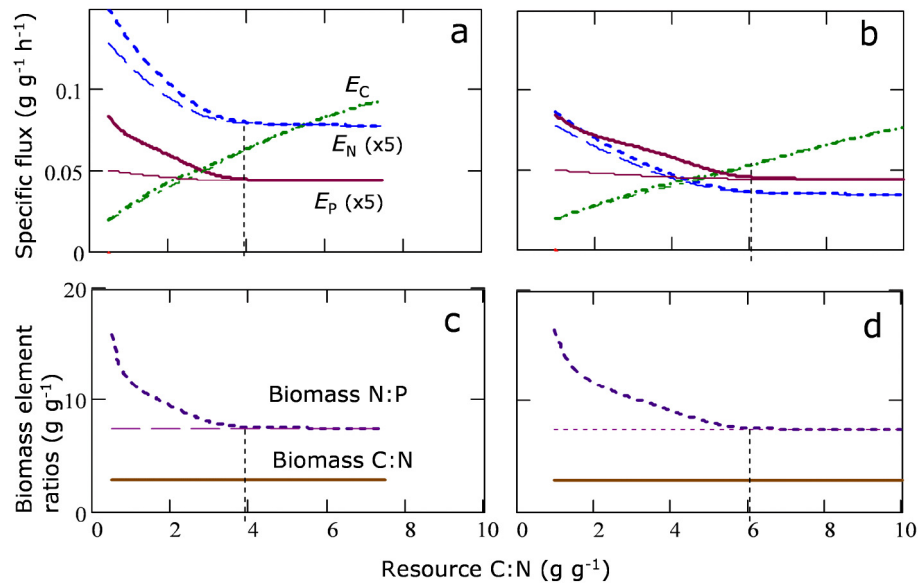


Fig. 4. Simulated C, N and P recycling (E_C , E_N , E_P) and bacterial (*P. carotovorum*) biomass element ratios in response to external resource C:N ratio. The difference between homeostatic structural biomass (thin lines) and dynamically optimized biomass partitioning (thick lines) was tested. Resource C:N was varied by reducing C availability from right to left on the x-axis, which caused a shift from N limitation to C limitation of bacterial growth (P was not limiting). The approximate shifting points are indicated by vertical dotted lines. **(a)** and **(b)**: Recycling (E) of C (dash-dot line), N x 5 (dashed line), and P x 5 (solid line). **(c)** and **(d)**: Structural biomass element ratios for C:N (solid line) and N:P(dashed line). **(a)** and **(c)** corresponds to double resource N level compared to **(b)** and **(d)**.

Implications for a microbial process –nutrient recycling

During microbial decomposition of organic matter, resource C:N and C:P ratios gradually decline due to the loss of C through microbial respiration. We evaluated the effect of our optimization hypothesis on this process for a bacteria (*P. carotovorum*) by model simulation of declining resource C level at two levels of fixed resource N availability and constant resource P (fig. 4).

Compared to if biomass was homeostatic, optimization of biomass composition led to a small increase in growth rate and a slight change in biomass C:N, but a significant change in biomass N:P when C limitation set in. More importantly, modeled recycling (mineralization) of both N and P was increased due to the optimization. This is explained by the shift from a low proportion of uptake machinery (u) under N limitation to higher u under C limitation (mechanism explained below). This shift increases uptake and therefore also excretion of excess non-limiting elements, i.e. P and N. If resource N level is reduced, the resource C:N ratio were the shift to C limitation occurs is increased. This effect of resource N level is due to the effect of maintenance respiration that causes a growth independent C use term, which means that total C use does not decline in proportion to N use as resource N level declines.

Discussion

Mechanisms regulating the contrasting biomass composition among P, N and C limitation

In both the model and the empirical studies, growth rate (G) scaled consistently with RNA and biomass P content under P limitation and under C limitation at higher growth rates, but not under N limitation. To understand these differences it is important to understand the two interacting mechanisms through which biomass partitioning maximizes growth rate in our model. First, changes in proportions of growth (g) and uptake machinery (u) cause a functional trade-off between growth and uptake capacity. Second, the resultant changes in biomass composition affect the demand for (use of) the limiting element per biomass constructed, i.e. a nutrient use efficiency effect (NUE effect) emerges. This effect determines the rate that the metabolite pool is depleted for a given growth rate (fig. 1b). While the functional trade-off always supports the GRH, the NUE effect does not. The NUE effect is important at low resource levels when it results in biomass patterns that are consistent with the GRH under P limitation but not under N limitation. Therefore, resource level ultimately determines which mechanism controls the relationship between biomass stoichiometry and growth.

The optimization of the functional trade-off acts equally for all limiting elements, by favoring growth machinery at the expense of uptake machinery as resource level increases. At high resource level this optimization of functional capacity is the dominant mechanism controlling biomass composition. Under these conditions the positive relationships between RNA, G and biomass P may emerge independent of which element is limiting, consistent with the GRH. Baseline biomass (z) will always be at its minimum value as it does not contribute to either uptake or growth capacity.

At declining resource level, the effect of uptake and growth capacity decline as uptake is controlled by resource level rather than uptake capacity (fig 1b, eq. 6). As a consequence, the relative importance of the NUE effect increases and biomass is allocated towards the compartment with the lowest concentration of the limiting nutrient. For example under P limitation, because uptake machinery is lowest and growth machinery highest in P the NUE effect reinforces the functional trade-off that reduces growth machinery as available P decreases. In contrast, under N limitation the NUE effect opposes the functional effect because growth machinery has lower N concentration than uptake machinery, leading to increasing allocation to growth machinery (RNA) even though growth rate is declining. However, at very low resource level increased baseline biomass (z) will be favored due to its even lower N concentration, despite that this reduces both uptake and growth capacity. Together these responses provide a mechanistic explanation for couplings between growth and biomass stoichiometry that lead to the non GRH compliant relationships observed under N limitation (fig. 2).

Under C limitation, there is an analogous but smaller NUE effect as under N limitation (because growth machinery is lower in C than uptake machinery). However, under C limitation, maintenance respiration becomes an important determinate of biomass C at low growth rate, which limits the importance of the NUE effect and maintains GRH compliant relationships except for very low growth rates (fig. 2).

Mechanisms regulating potential sub-optimal variability in biomass composition

The modeled differences in the near optimal ranges (the distance between the thin lines in fig. 2) under limitation by different nutrients suggests that the relationship between optimized g and the specific growth rate (and therefore the RNA – G relationship) is much less constrained and more prone to variation at low G under C limitation and under N limitation, than under P limitation. For example, the near optimal range of RNA: protein is ≈ 10 times larger under N than under P limitation at low growth rate for *P. carotovorum* (fig.

2). This difference is due to the interaction of the NUE effect and functional effect on the optimal biomass allocation. Under P limitation these mechanisms work together, amplifying the effect of P use on growth, whereas under N limitation they oppose each other and therefore tend to cancel out. This difference leads to a high sensitivity of G to P use and therefore to variation in biomass composition (g and z) under P limitation, while under N limitation the corresponding sensitivity of G to biomass composition is low.

Novel aspects and implications for microbial biomass stoichiometry

Our model links physiology directly to biomass composition and therefore to biomass stoichiometry, employing optimization of structure composition as the controlling mechanism. We have shown that the optimization strategy, rooted in an ecological and evolutionary rationale, provides a means to understand how microbial biomass stoichiometry and physiology is influenced by changes in the environment, including resource variation. In addition to the novel optimization strategy, our model differs from widely used microbial stoichiometry models (e.g. quota models, Droop 1968; Thingstad 1987) in its more mechanistic representation of the growth process that describes gradual shifts between different resource limitations and the explicit interaction of growth machinery and metabolite pools. Supported by empirical data we showed how this interaction leads to a positive concave relationship between G and the metabolite pool for a limiting nutrient, while the metabolite pool tend to decrease with G at high G for non-limiting nutrients (fig. 3). Our model provides a mechanistic explanation for such relationships, which also have been observed for different nutrients in yeast (Boer et al. 2010).

We applied the model to elucidate observed patterns of covariation among biomass composition, stoichiometry and growth, such as the growth rate hypothesis (GRH) under different resource stoichiometry. Integration of stoichiometric theory, cellular composition and physiology has previously been done based on the GRH (Vrede et al. 2004) and by incorporating the GRH into the metabolic theory of ecology (Allen and Gillooly 2009). However, while the resulting theory explained patterns across organism types it did not explain how individual organisms and populations adapt or acclimate to changes in resource level and stoichiometry. Contrastingly, adaptive phenotypic plasticity, i.e. optimal acclimation of biomass composition, is central in our model. Moreover, multiple empirical studies show that a theory where ribosome content always correlates with growth seems insufficient for dealing with microorganisms as they often defy the GRH under non P limitation (Binder and Liu 1998; Elser et al. 2003;

Flärdh et al. 1992). In the light of our model such results are explained by opposing effects of biomass composition on functional capacities versus nutrient use efficiency, exemplified for *P. carotovorum* under N limitation (fig. 2). In addition, at low G under C- and particularly N limitation, our model implies that G is relatively insensitive to variation in cell composition (fig. 2) suggesting an explanation for the high variability in stoichiometric relationships and RNA observed under these conditions. Thus, our model offers a mechanistic explanation for observations of variable and high RNA abundance at low G , which has previously been suggested to be a means of responding quickly to increased resource level (Flärdh et al. 1992). Our suggested mechanism may also have contributed to the decoupling of growth rate RNA and biomass P observed in bacteria across a large number of lakes (Hall et al. 2009).

Although our results are consistent with the limited validity of the GRH observed under many resource conditions they do not imply that the GRH is exclusively restricted to P limitation as suggested by Elser et al. (2003). We showed that organisms grown under C limitation (*E. coli*, fig. 2) can give rise to a similar relationship between G and RNA as under P limitation. However, in contrast to P limitation, under C limitation such relationships result from a purely functional trade-off between uptake and growth capacity and not affected by nutrient (here C) use efficiency. Although not shown, the functional trade-off also leads to GRH compliant relationships under “balanced growth”, i.e. when all nutrients are co-limiting, because there is no opposing effect of nutrient use efficiency (NUE) as there is no benefit of increasing NUE of any particular nutrient relative to other nutrients. In agreement with these predictions, the GRH has been verified for a range of microorganisms under balanced growth or C limitation (Karpinets et al. 2006).

The relationship between RNA and G varied significantly between *E. coli* and *P. carotovorum* (fig. 2), supporting empirical results that show that this relationship is stronger within a species than across species (Kemp et al. 1993; Kerkhof and Kemp 1999) or communities (Hall et al. 2009). Furthermore, our model implies that this relationship is strongly linked to the capacity of the growth machinery, i.e. the maximal synthetic capacity of RNA (f_G ; eqs. 3-5), which differs strongly between our investigated species (Table 2). This result explains mechanistically why the synthetic capacity of rRNA is a key factor controlling differences in the RNA - G relationship across species with different ecological strategies, as has been proposed (Dethlefsen and Schmidt 2007). These inter-species differences may also be reinforced by differences in the proportion of biomass not related to growth or uptake

(z), which we predicted to be much higher for the slower growing *P. carotovorum* than the fast growing *E. coli*.

Implications for nutrient cycling

Nutrient recycling (mineralization) is in large part a microbial process which is strongly affected by the stoichiometry of microbial biomass (Cherif and Loreau 2007; Manzoni et al. 2008). Because our growth mechanism (eq. 3) is based on the synthesizing unit concept (Kooijman 1998, Kooijman 2001) it readily models the gradual shift from N to C limitation of microbial growth that gradually enhances the N (and P) mineralization: immobilization ratio during the decomposition process. Our results indicate that the excretion of N and P during organic matter decomposition is increased if biomass is dynamically optimized compared to if it was strictly homeostatic. Therefore, our model results suggest that part of nutrient mineralization during organic matter decomposition is a by-product of microorganisms adjusting their biomass composition to maximize growth (fig. 4). Thus, our suggested optimization mechanism may allow us to develop a better understanding of nutrient mineralization and immobilization dynamics in ecosystems.

Limitations and possibilities for additional evaluation

Our ability to validate all aspects of the model for a wider range of microorganisms was limited by the availability of data that included all necessary biomass compartments, growth rate, and a conclusive identification of the limiting nutrient. In particular, direct evidence for changes in uptake capacity would be valuable for additional testing of the model and the potential effects on nutrient recycling. However, while the link between growth machinery and RNA is well established, a measure of uptake machinery is not readily obtainable from macromolecular composition. However, the application of stable isotope probing and single cell techniques to microbial ecology may allow for higher resolution and more specific estimates uptake dynamics in future studies (Wagner 2009).

Although our data supports our assumption that the metabolite pools are in equilibrium with the growth rate (fig. 3) this may not always be the case, for example under rapid variations in resource level. However, if the equilibrium assumption (eq. 2) is relaxed the model should also be valid under non equilibrium conditions, which would be an interesting topic for further analysis.

Conclusions

Our analysis suggests that maximization of specific growth rate (G) constrained by a trade-off between growth and uptake capacity is a dominant control on bacterial biomass composition. In addition, the shifts in biomass composition affects the resource demands for a given growth rate, i.e. nutrient use efficiency, because the elemental composition of each cellular component is unique. These two mechanisms can be complementary as under P-limitation and strengthen the relationship between growth and biomass stoichiometry. They can also act antagonistically, for example under N limitation. At low resource level, where nutrient use efficiency becomes a more important control than the functional growth - uptake trade-off the nutrient use efficiency optimization will lead to different biomass allocation patterns depending on which nutrient is limiting. For example that the growth rate hypothesis (GRH) is valid under P limitation but breaks down under N limitation. The elucidation of these specific mechanisms provides the first clear mechanistic explanation for why GRH relationships can come uncoupled under certain resource stoichiometry. In addition, the model results suggest that optimization of cellular composition during decomposition of organic matter indirectly increases N and P mineralization. Such dynamics may play an important role in nutrient cycling in ecosystems.

The ability of the model to mechanistically predict bacterial biomass stoichiometry and the model's potential implications for nutrient recycling suggest that its mechanisms may be an appropriate starting point for incorporating dynamic microbial physiology into ecosystem level models. Because our model is rooted in an ecological and evolutionary rationale it can be used to mechanistically explain patterns of microbial stoichiometry in an ecological context. In addition to established empirical patterns of what happens (e.g. biomass P:N ratio increases with G), the model explains when it happens (e.g. under C limitation), how it happens (e.g. growth-uptake trade-off), and why it happens (ecological optimization).

Acknowledgements

This work is a contribution from the Austrian national research network MICDIF and was supported by the Austrian Science Foundation (FWF, S1001-B07) and IIASA, International Institute of Applied Systems Analysis.

References

- Allen, A. P., and J. F. Gillooly. 2009. Towards an integration of ecological stoichiometry and the metabolic theory of ecology to better understand nutrient cycling. *Ecology Letters* 12:369–384.
- Bergey, D. H., F. C. Harrison, R. S. Breed, B. W. Hammer, and F. M. Huntoon. 1923. Pages 374–375 *Bergey's manual of determinative bacteriology*, The Williams & Wilkins Co., Baltimore.
- Binder, B. J., and Y. C. Liu. 1998. Growth rate regulation of rRNA content of a marine *Synechococcus* (cyanobacterium) strain. *Applied and Environmental Microbiology* 64:3346–3351.
- Boer, V. M., C. A. Crutchfield, P. H. Bradley, D. Botstein, and J. D. Rabinowitz. 2010. Growth-limiting intracellular metabolites in yeast growing under diverse nutrient limitations. *Molecular Biology of the Cell* 21:198–211.
- Brandt, B. W., F. D. L. Kelpin, I. M. M. Van Leeuwen, and S. A. L. M. Kooijman. 2004. Modelling microbial adaptation to changing availability of substrates. *Water Research* 38:1003–1013.
- Cajal-Medrano, R., and H. Maske. 1999. Growth efficiency, growth rate and the remineralization of organic substrate by bacterioplankton - Revisiting the Pirt model. *Aquatic Microbial Ecology* 19:119–128.
- Cherif, M., and M. Loreau. 2007. Stoichiometric constraints on resource use, competitive interactions, and elemental cycling in microbial decomposers. *American Naturalist* 169:709–724.
- Chrzanowski, T. H., and J. P. Grover. 2008. Element content of *Pseudomonas fluorescens* varies with growth rate and temperature: A replicated chemostat study addressing ecological stoichiometry. *Limnology and Oceanography* 53:1242–1251.
- Chrzanowski, T. H., and M. Kyle. 1996. Ratios of carbon, nitrogen and phosphorus in *Pseudomonas fluorescens* as a model for bacterial element ratios and nutrient regeneration. *Aquatic Microbial Ecology* 10:115–122.
- Clark, D. J., and O. Maaloe. 1967. DNA Replication and Division Cycle in *Escherichia Coli*. *Journal of Molecular Biology* 23:99–112.
- Dethlefsen, L., and T. M. Schmidt. 2007. Performance of the translational apparatus varies with the ecological strategies of bacteria. *Journal of Bacteriology* 189:3237–3245.
- Droop, M. R. 1968. Vitamin B12 and marine ecology, IV. The kinetics of uptake, growth and inhibition in *Monochrysis lutheri*. *J. Mar. Biol. Assoc. UK* 48:689–733.
- Elser, J. J., K. Acharya, M. Kyle, J. Cotner, W. Makino, T. Markow, T. Watts et al. 2003. Growth rate-stoichiometry couplings in diverse biota. *Ecology Letters* 6:936–943.
- Elser, J. J., M. M. Kyle, M. S. Smith, and J. D. Nagy. 2007. Biological stoichiometry in human cancer. *PLoS ONE* 2.
- Ferenci, T. 2007. *Bacterial Physiology, Regulation and Mutational Adaptation in a Chemostat Environment*, *Advances in Microbial Physiology*.
- Flårdh, K., P. S. Cohen, and S. Kjelleberg. 1992. Ribosomes exist in large excess over the apparent demand for protein synthesis during carbon starvation in marine *Vibrio* sp. strain CCUG 15956. *Journal of Bacteriology* 174:6780–6788.
- Franklin, O., R. E. McMurtrie, C. M. Iversen, K. Y. Crous, A. C. Finzi, D. T. Tissue, D. S. Ellsworth et al. 2009. Forest fine-root production and nitrogen use under elevated CO₂: Contrasting responses in evergreen and deciduous trees explained by a common principle. *Global Change Biology* 15:132–144.
- Gelman, A., J. B. Carlin, H. S. Stern, and D. B. Rubin. 2004. *Bayesian Data Analysis*, Chapman & Hall, CRC.
- Hall, E. K., A. R. Dzialowski, S. M. Stoxen, and J. B. Cotner. 2009. The effect of temperature on the coupling between phosphorus and growth in lacustrine bacterioplankton communities. *Limnology and Oceanography* 54:880–889.
- Jackson, J. H., T. M. Schmidt, and P. A. Herring. 2008. A systems approach to model natural variation in reactive properties of bacterial ribosomes. *BMC Systems Biology* 2.
- Karpinets, T. V., D. J. Greenwood, C. E. Sams, and J. T. Ammons. 2006. RNA: Protein ratio of the unicellular organism as a characteristic of phosphorous and nitrogen stoichiometry and of the cellular requirement of ribosomes for protein synthesis. *BMC Biology* 4.
- Keiblinger, K. M., E. K. Hall, W. Wanek, U. Szukics, I. Hämmerle, G. Ellersdorfer, S. Böck et al. 2010. The effect of resource quantity and resource stoichiometry on microbial carbon use efficiency. *FEMS Microbiology Ecology*. DOI: 10.1111/j.1574-6941.2010.00912.x
- Kemp, P. F., S. Lee, and J. LaRoche. 1993. Estimating the growth rate of slowly growing marine bacteria from RNA content. *Applied and Environmental Microbiology* 59:2594–2601.
- Kerkhof, L., and P. Kemp. 1999. Small ribosomal RNA content in marine Proteobacteria during non-steady-state growth. *FEMS Microbiology Ecology* 30:253–260.
- Klausmeier, C. A., E. Litchman, T. Daufreshna, and S. A. Levin. 2004. Optimal nitrogen-to-phosphorus stoichiometry of phytoplankton. *Nature* 429:171–174.
- Kolmer, J. A., E. H. Spaulding, and H. W. Robinson. 1951. Pages 1090–1091 *Approved Laboratory Techniques*, Appleton Century Crafts, New York.

- Kooijman, S. A. L. M. 1998. The Synthesizing Unit as model for the stoichiometric fusion and branching of metabolic fluxes. *Biophysical Chemistry* 73:179-188.
- . 2001. Quantitative aspects of metabolic organization: A discussion of concepts. *Philosophical Transactions of the Royal Society B: Biological Sciences* 356:331-349.
- Kozlowski, J., M. Czarnoleski, and M. Danko. 2004. Can optimal resource allocation models explain why ectotherms grow larger in cold? *Integrative and Comparative Biology* 44:480-493.
- Leser, T. D., M. Boye, and N. B. Hendriksen. 1995. Survival and activity of *Pseudomonas* sp. strain B13(FR1) in a marine microcosm determined by quantitative PCR and an rRNA-targeting probe and its effect on the indigenous bacterioplankton. *Applied and Environmental Microbiology* 61:1201-1207.
- Makino, W., and J. B. Cotner. 2004. Elemental stoichiometry of a heterotrophic bacterial community in a freshwater lake: Implications for growth- and resource-dependent variations. *Aquatic Microbial Ecology* 34:33-41.
- Makino, W., J. B. Cotner, R. W. Sterner, and J. J. Elser. 2003. Are bacteria more like plants or animals? Growth rate and resource dependence of bacterial C:N:P stoichiometry. *Functional Ecology* 17:121-130.
- Manzoni, S., R. B. Jackson, J. A. Trofymow, and A. Porporato. 2008. The global stoichiometry of litter nitrogen mineralization. *Science* 321:684-686.
- Pirt, S. J. 1982. Maintenance energy: a general model for energy-limited and energy sufficient growth. *Archives of Microbiology* 133:300-302.
- Prosser, J. I., B. J. M. Bohannan, T. P. Curtis, R. J. Ellis, M. K. Firestone, R. P. Freckleton, J. L. Green et al. 2007. The role of ecological theory in microbial ecology. *Nature Reviews Microbiology* 5:384-392.
- Raman, B., M. P. Nandakumar, V. Muthuvijayan, and M. R. Marten. 2005. Proteome analysis to assess physiological changes in *Escherichia coli* grown under glucose-limited fed-batch conditions. *Biotechnology and Bioengineering* 92:384-392.
- Russell, J. B., and G. M. Cook. 1995. Energetics of bacterial growth: Balance of anabolic and catabolic reactions. *Microbiological Reviews* 59:48-62.
- Schinner, F., R. Ählinger, E. Kandeler, and R. Margesin. 1993. *Bodenbiologische Arbeitsmethoden*. Vol 2. Auflage., Springer Labor.
- Sepers, A. B. J. 1986. Effect of variable nutrient supply rates on the RNA level of a heterotrophic bacterial strain. *Current Microbiology* 13:333-336.
- Sterner, R. W. 1995. Elemental stoichiometry of species in ecosystems, Pages 240-252 *in* C. Jones, and J. Lawton, eds. *Linking Species and Ecosystems*. New York, NY, Chapman and Hall.
- Sterner, R. W., and J. J. Elser. 2002. *Ecological Stoichiometry: The Biology of Elements from Molecules to the Biosphere*. Princeton, Princeton University Press.
- Tännler, S., S. Decasper, and U. Sauer. 2008. Maintenance metabolism and carbon fluxes in *Bacillus* species. *Microbial Cell Factories* 7.
- Thingstad, F. 1987. Utilization of N, P and organic C by heterotrophic bacteria I. Marine ecology - Progress series 35:99-109.
- Thomas, M. R., and E. K. O'Shea. 2005. An intracellular phosphate buffer filters transient fluctuations in extracellular phosphate levels. *Proceedings of the National Academy of Sciences of the United States of America* 102:9565-9570.
- Van Bodegom, P. 2007. Microbial maintenance: A critical review on its quantification. *Microbial Ecology* 53:513-523.
- Vrede, T., D. R. Dobberfuhl, S. A. L. M. Kooijman, and J. J. Elser. 2004. Fundamental connections among organism C:N:P stoichiometry, macromolecular composition, and growth. *Ecology* 85:1217-1229.
- Wagner, M. 2009. Single-cell ecophysiology of microbes as revealed by Raman microspectroscopy or secondary ion mass spectrometry imaging. *Annual Review of Microbiology* 63:411-429.
- Wirtz, K. W. 2002. A generic model for changes in microbial kinetic coefficients. *Journal of Biotechnology* 97:147-162.

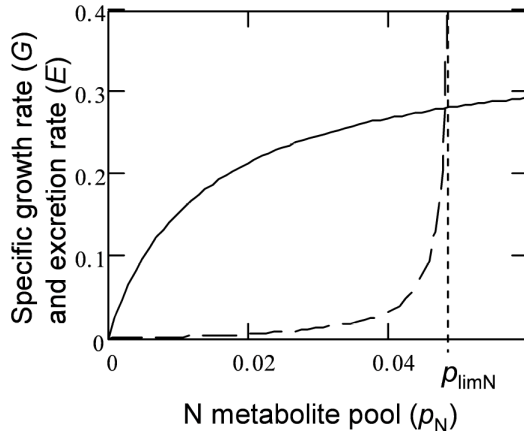
Appendix A - The synthesizing unit (SU) and growth

A SU is analogous to an enzyme where substrate molecules bind to form a product that is then released (Kooijman 1998, Kooijman 2001). In our case the product is biomass and the substrates are carbon (C), nitrogen (N) and phosphorus (P) (all other atoms in biomass and substrate are implicit). The SU has binding sites for all substrate molecules, where all sites must bind substrate before the product is released. The production rate of the SU depends on the probabilities per time unit that the substrate molecules bind (substrate flux) relative to the number of binding sites. In our model, the relative number of binding sites among elements in the SU mirrors the content of the elements in biomass (b_x). The substrate flux (binding probability) is proportional to the metabolite concentrations for each nutrient (p_x). This formulation is based on the SU model simplified for production of a generalized compound

(biomass) limited by three substrates (C, N, P) (Kooijman 1998).

The above describe the growth properties per unit growth machinery (corresponding to one SU). To incorporate the effects of variable amounts of growth machinery (many SUs), we apply basic Michaelis-Menten type kinetics. At low amounts of growth machinery relative to p , specific growth (G) is limited by G_{max} (eq. 4), which is proportional to the amount of growth machinery ($g(1-z)$) and its maximum capacity of biomass synthesis (f_G), which is a function of the maximal translational activity of the ribosomes (cf. (Jackson et al. 2008)). At high amounts of growth machinery relative to metabolite concentration, many units of growth machinery compete for little substrate so that G is not limited by the amount of growth machinery but by its efficiency (e_g), i.e. product formation of each SU per nutrient flux.

Online Appendix B – Fig B1



Online Fig B1. Modeled microbial growth (solid line) and excretion (dashed line) as a function of internal nutrient metabolite pool (p_N). Excretion prevents p_N to exceed the maximum $p_N = p_{limN}$ (dotted vertical line).

Online Appendix C – Experiment for *Pectobacterium carotovorum*

Treatments

Pectobacterium carotovorum (Bergey et al. 1923) was cultivated in batch cultures, in three replicates, in liquid minimal media modified from (Clark and Maaloe

1967). The media contained MOPS 30 mM pH 7.0, CaCl_2 0.1 mM, FeSO_4 3 μM , KCl 20 mM, MgCl_2 2 mM, Na_2SO_4 14 mM, NaCl 51 mM. Glucose, NH_4Cl and Na_2HPO_4 were added as carbon (C), nitrogen (N) and phosphorus (P) sources in different amounts and ratios, giving a total of 12 combinations (12 treatments) of C, N and P. Bacterial media were sterilized by autoclaving at 121°C for 20 min. Glucose was added to autoclaved media from filter-sterilized (pore size 0.2

µm) stock solutions. The inoculation on the media was made from pre-culture grown for 60 h in the respective minimum media with fixed concentrations of 150 mM C, 12.5 mM N, and 0.25 mM P. The pre-culture was then centrifuged; the pellet was washed twice with minimal media without C, N or P sources and then once more re-suspended in minimal media to inoculate the 12 treatments. Cultivation was performed in 400 mL medium at 22°C on a rotary shaker with 180 rpm. For determination of biomass and its elemental composition, each of the 12 treatments was run in 400 ml either three or four replicates as mentioned above. For each treatment the bacterial cultures were measured at two growth phases, logarithmic (initial fast growth) and stationary phase (late slow, strongly resource limited growth).

Measurements

The bacterial cultures were transferred into centrifuge flasks and centrifuged for 45 min at 10845 g. The biomass pellet was washed twice with 50 ml 130 mM NaCl, followed by resuspension in 50 mL 130 mM NaCl and centrifugation for 10 minutes at 10845 g. The biomass was dried in a drying oven for determination of dry mass, C, N and P content. Aliquots of dried biomass (~2 mg) were weighed into tin capsules and total C and N were determined with an elemental analyzer (EA 1110, CE Instruments, Milan, Italy). For analysis of total P in biomass, approximately 10 mg of dried samples were wet digested with 1 ml nitric acid-perchloric acid mixture (HNO₃:HClO₃ 4:1; (Kolmer et al. 1951) in 2 mL glass flasks on a heating plate. For acid digestion the temperature was increased stepwise to 250 °C and keeping the temperature until a small residual volume was left in the glass flask. Samples were cooled to room temperature, and filled up to the 2 ml with milliQ water. Inorganic P in the digests was quantified photometrically based on the phosphomolybdate blue reaction (Schinner et al. 1993)

in a microtiter plate format with a Microplate Reader (BIO-TEK Instruments, Inc.). RNA content was measured by fluorometry using the fluorescent stain RiboGreen® after the methods of (Makino and Cotner 2004). The growth rates were determined by measuring the increase in turbidity. Turbidity was monitored at regular interval with a Microplate reader with 250 µL aliquots at a wavelength of 450 nm for bacteria. Optical density (OD) growth kinetics was constructed by plotting OD of suspensions corrected for non-inoculated medium vs. time of incubation. At biomass densities higher than OD>0.6 the samples were diluted.

Calculation of growth rate and identification of limiting resource

The bacterial growth rate was determined using a five parameter logistic growth model, which was fitted (using the Levenberg-Marquardt algorithm in the software SigmaPlot) to measured OD as a function of time. Specific growth rate (G) was evaluated for each biomass sampling point t_s as growth in OD divided by OD, i.e. $G = ((dOD/dt) / OD)$ at $t = t_s$. Observations at extremely low growth rates, not significantly different from zero were excluded due to the high uncertainty in the growth rate estimate.

The change in non-nucleic acid P ($P_{total} - P_{RNA} - P_{DNA} \approx$ non-structural, metabolite P) with growth rate between the two growth phases were used to detect the limiting resource. P limitation was indicated (according to our theory) by decreased non-nucleic acid P concentration during the transition from initial (fast) to late (slow) growth. The results were also confirmed by an analysis of polyphosphate (indicative of P storage). Absence of P limitation was interpreted as N limitation. C limitation was excluded because carbohydrate concentration (indicating C storage) increased between logarithmic and stationary phase in all treatments.